

Design Algorithm of Harmonic Filters in a Meshed Transmission Grid with Distributed Harmonic Emission Sources – Eastern Danish Transmission Grid Case Study

Akhmatov, Vladislav; Sørensen, Mikkel; Jakobsen, Troels; Hansen, Chris Skovgaard ; Gellert, Bjarne Christian; Bukh, Bjarne Søndergaard

*Published in:*  
Proceedings of 21st Wind & Solar Integration Workshop

*Creative Commons License*  
CC BY 4.0

*Publication date:*  
2022

*Document Version*  
Publisher's PDF, also known as Version of record

[Link to publication from Aalborg University](#)

*Citation for published version (APA):*

Akhmatov, V., Sørensen, M., Jakobsen, T., Hansen, C. S., Gellert, B. C., & Bukh, B. S. (2022). Design Algorithm of Harmonic Filters in a Meshed Transmission Grid with Distributed Harmonic Emission Sources – Eastern Danish Transmission Grid Case Study. In *Proceedings of 21st Wind & Solar Integration Workshop* Energynautics GmbH.

**General rights**

Copyright and moral rights for the publications made accessible in the public portal are retained by the authors and/or other copyright owners and it is a condition of accessing publications that users recognise and abide by the legal requirements associated with these rights.

- Users may download and print one copy of any publication from the public portal for the purpose of private study or research.
- You may not further distribute the material or use it for any profit-making activity or commercial gain
- You may freely distribute the URL identifying the publication in the public portal -

**Take down policy**

If you believe that this document breaches copyright please contact us at [vbn@aub.aau.dk](mailto:vbn@aub.aau.dk) providing details, and we will remove access to the work immediately and investigate your claim.



# DESIGN ALGORITHM OF HARMONIC FILTERS IN A MESHED TRANSMISSION GRID WITH DISTRIBUTED HARMONIC EMISSION SOURCES – EASTERN DANISH TRANSMISSION GRID CASE STUDY

*Vladislav Akhmatov<sup>1\*</sup>, Mikkel Sørensen<sup>1</sup>, Troels Jakobsen<sup>1</sup>, Chris Liberty Skovgaard<sup>1</sup>,  
Bjarne Christian Gellert<sup>1</sup>, Bjarne Søndergaard Bukh<sup>1,2</sup>*

<sup>1</sup>*Energinet, Transmission System Operator of Denmark, Fredericia, Denmark*

<sup>2</sup>*AAU Energy, Aalborg University, Denmark*

*\*vla@energinet.dk*

**Keywords:** HARMONIC DISTORTION, HARMONIC FILTER, MESHED TRANSMISSION GRID, SIMULATION, VALIDATION

## Abstract

The transmission grid in Denmark undergoes tremendous reinforcement and development due to massive integration of renewables and PtX, stronger market coupling with foreign grids and connection of the Energy Islands. The political goal is that new transmission lines shall, to the most technically feasible extent, be established as underground cables (UGC) and part of overhead lines (OHL) substituted with UGC. The Danish experience has shown that especially 400 kV UGC may cause resonance conditions, which coincide with harmonic orders of the harmonic distortion and increase the harmonic voltage distortion. Establishment of harmonic filters with the right properties, ratings and locations in the transmission grid is among mitigation solutions of excessive harmonic distortion. In the meshed transmission grid, a new harmonic filter may, on the one hand, dampen a specific harmonic order in the given substation, but, on the other hand, become inefficient or even increase harmonic distortion in other substations. Therefore, the harmonic filter design for the meshed transmission grid is a challenging task. This presentation will explain the algorithm developed by Energinet, Transmission System Operator of Denmark, for automated design of harmonic filters in the meshed transmission grids by simulations. The algorithm will be demonstrated using a validated simulation model of the Eastern Danish 400 kV transmission grid for harmonic assessment as a case study.

## 1 Abbreviations

DKE	Eastern Denmark (Transmission Grid)
DKW	Western Denmark (Transmission Grid)
HVAC	High Voltage Alternating Current
HVDC	High Voltage Direct Current
LCC	Line Commutated Converter
OHL	Overhead Line
PQ	Power Quality
SCADA	Supervisory Control and Data Acquisition
SE4	Market Zone 4 of the transmission grid of Sweden
SvK	Svenska Kraftnät, Transmission System Operator of Sweden
STATCOM	Stationary (Nonrotating) Compensator
VSC	Voltage Source Converter
UGC	Underground Cable

### 1.1 HVAC substations

The 400 kV substations in Eastern Denmark.

ASV	Asnæs	HCV	H. C. Ørsted Værket
AVV	Avedøre	HKS	Herslev
BJS	Bjæverskov	HVE	Hovegård
GLN	Glentegård	ISH	Ishøj
GØR	Gørlose		

The 400 kV substations in Sweden with relevance for the presentation.

SÅNS	Söderåsen
------	-----------

### 1.2 HVDC connections and converter stations

The HVDC converter stations in Eastern Denmark (LCC).

KO	Kontek (600 MW, BJS, DKE – Germany)
SB	Storebælt (600 MW, HKS, DKE – DKW)

The HVDC converter stations in Sweden with relevance for the presentation (LCC).

BA	Baltic Cable (600 MW, AIES, Sweden – Germany)
----	---

KS1	Konti-Skan 1 (370 MW, LDOS 400 kV, Sweden – DKW)
KS2	Konti-Skan 2 (370 MW, LDOS 132 kV, Sweden – DKW)
SP	SwePol (600 MW, STÖS, Sweden – Poland)

## 2 Introduction

Accelerated green transition of the energy sectors increases the share of converter-interfaced electricity production, consumption, and storages, and enables significant expansion and development of the transmission grid. The green transition may lead to evolution of the harmonic emission sources due to more converter-interfaced units and altering the harmonic impedance characteristics and resonances in the different substations of the grid due to development of the electricity infrastructure.

Motivated by principles for developing the electricity infrastructure in Denmark, which is defined in the political agreement from October 2020, the share of UGC in the Danish transmission grid is increasing [1].

In simple terms, the resonance frequency of the grid is expressed by  $f_n = 1/(2\pi \cdot (L \cdot C)^{1/2})$ , with  $L$  being frequency dependent. The resonance frequency,  $f_n$ , will decrease when the share of UGC increases because more UGC in-service increase the capacitance of the grid,  $C$ . The resonance frequency of the meshed grid,  $f_n$ , may increase when the share of OHL in-service increases. Specifically for the meshed grid, the OHL connections can be considered in parallel operation reducing the inductance of the grid,  $L$ .

In general terms, the harmonic impedance characteristics have several peaks (resonances) and valleys corresponding to specific combinations of capacitances and inductances of the different connections, transformers, and harmonic filters in-service. The harmonic impedance characteristics are not identical in different substations of the meshed transmission grid. Following the above discussion on the resonance frequency,  $f_n$ , introduction of more UGC will shift the harmonic impedance resonances (peaks) to lower harmonic orders, while more OHL in-service in the meshed grid may shift the harmonic impedance resonances to higher harmonic orders.

In contrast to the OHL connections in parallel operation within “bulk” meshed grids, establishment of radial OHL connections will increase the inductance,  $L$ , so that lowering resonance frequencies of the harmonic impedance characteristics in the adjacent substations. Radial UGC connections will lower resonance frequencies of the harmonic impedance characteristics in the adjacent substations due to increasing the capacitance,  $C$ .

For the Danish 400 kV transmission grid, the characteristic orders of the harmonic distortion are the 3<sup>rd</sup>, 5<sup>th</sup>, 7<sup>th</sup>, 11<sup>th</sup>, 13<sup>th</sup>, 23<sup>rd</sup> and 25<sup>th</sup> [1], [2]. Establishment of the 400 kV UGC has

already brought the harmonic impedance resonances (peaks) down within the harmonic order ranges coinciding the harmonic distortion and causing increase of the harmonic voltage distortion. For example, a double 400 kV UGC system of Vejle-Ådal in the Western Danish transmission grid, 7 km line length, substituting an OHL and energized in July 2017, has resulted in significant increase of the 11<sup>th</sup> and 13<sup>th</sup> harmonic voltage distortion originating from the HVDC converter stations [3].

Reinforcement of the Danish transmission grid using more UGC will further lower the resonance frequencies of the harmonic impedance characteristics so that more peaks of the harmonic impedance characteristics may appear within the harmonic order ranges coinciding the background harmonic distortion and increasing risks of its amplification. When the resonances are changed to other frequencies, their magnitudes are also changed.

The harmonic resonances in the meshed grid are not only influenced by newly established connections but also by  $(n-M)$ ,  $M \geq 0$ , operation conditions with  $M$  referring to transmission lines, transformers, and harmonic filters out-of-service. The  $(n-M)$  operation conditions alter the share of capacitances,  $C$ , and inductances,  $L$ , shifting the resonance frequencies and magnitudes of the harmonic impedance characteristics.

Excessive harmonic voltage distortion can be mitigated using harmonic filters with right design parameters and connected to right substations in the grid. From the above discussion, it becomes clear that proper design of harmonic filters in the meshed transmission grid can be a challenging task. Incorrect design may result in:

- The harmonic filter may dampen harmonic distortion in some substations and, at the same time, be inefficient or even increase harmonic distortion in other substations [4].
- The harmonic filter may dampen harmonic distortion in a range of its tuning order but increase harmonic distortion of other harmonic orders [4].

The above outcomes can be present because:

- The harmonic filter may shift resonance frequencies and magnitudes of the harmonic impedance characteristics in several substations of the meshed transmission grid.
- Various  $(n-M)$ ,  $M \geq 0$ , operation regimes may shift the harmonic impedance characteristics in such a manner that reduces dampening characteristics of the harmonic filter or even increases the harmonic distortion (other harmonic orders and/or in other substations).

This paper will describe a mathematical algorithm developed by Energinet for automated design of harmonic filters in meshed transmission grids with several harmonic sources. The algorithm will be demonstrated by simulations of the harmonic voltage distortion using a validated model of the Eastern Danish 400 kV transmission grid [1] with establishment of a new 400 kV UGC as a case study. Finally, the paper will outline potentials of the algorithm for design,

control, and operation of active filters, and future trends on design of harmonic filters.

### 3 Harmonic filter design algorithm

Consider a meshed transmission grid area with  $S$  substations. The magnitudes of the background harmonic distortion of the harmonic order  $k$  are acquired from the PQ measurements or simulations.

Different  $(n-M)$ ,  $M \geq 0$ , operation conditions of the grid with transmission lines, transformers and existing harmonic filters out-of-service combined with different power transports result in the different operation scenarios. The different operation scenarios may have different magnitudes of the harmonic voltage distortion which in the algorithm is denoted by the scenario index  $p = 1 \dots P$ .

Regarding the evaluation practice for maintaining the  $k^{\text{th}}$  harmonic performance criteria,  $U_{PL,k}$ , the algorithm may apply either the maximum, the average, or the positive (negative, zero) sequence of the harmonic voltage magnitudes in the three phases,  $U_{p,s,k}$ , with the substation index  $s = 1 \dots S$ .

For the Danish transmission grid, the maximum of the 10-minute values of the harmonic voltage magnitudes in the three phases will be applied. The performance criteria for the filter design will be the IEC planning levels  $U_{IEC,k}$  [5] multiplied by a margin,  $f_{PL,k}$ , which is usually below 100%. The Danish practice accounts also for the filter component tolerances,  $\delta_{TOL}$ , such as the manufacturing and operational (temperature variation) tolerances [6]. Thus, the performance criteria become:

$$U_{PL,k} = U_{IEC,k} f_{PL,k} (1 - \delta_{TOL}). \quad (1)$$

A successful design of the harmonic filter shall result in the harmonic voltage magnitudes of all the harmonic orders  $k$  in the  $S$  substations comply with:  $U_{p,s,k} < U_{PL,k}$ ,  $s = 1 \dots S$ .

The design parameters of harmonic filters are the rated reactive power,  $Q_{HF}$  (MVar), nominal voltage,  $U_{HF}$  (kV), nominal frequency,  $f_{HF}$  (Hz), harmonic tuning orders,  $n_h$ , and quality factor  $q_F$ . The nominal voltage,  $U_{HF}$ , and frequency,  $f_{HF}$ , are locked on the transmission grid and equipment standards applied by the grid operator. The rated reactive power,  $Q_{HF}$ , harmonic tuning orders,  $n_h$ , and quality factor,  $q_F$ , are to be defined by the filter design algorithm.

First, the main definitions and mathematical expressions of the algorithm will be given. Then, the design process will be explained referring to the definitions and expressions, first for the different operation scenarios one by one,  $p$ , and, then, complying with all included operation scenarios,  $p = 1 \dots P$ .

#### 3.1 Substation groups

The substations of the transmission grid area, where the harmonic filter shall dampen excessive harmonic voltage distortion, is divided into the two groups:

- The first group,  $s1$ , includes the substations  $s = 1 \dots s1$  where the harmonic filter shall maintain the harmonic voltage magnitudes  $U_{p,s,k}$  below the performance criteria,  $U_{PL,k}$ . Mitigation of excessive harmonic voltage distortion in the substation group  $s1$  is the primary target of the harmonic filter design.
- The second group,  $s2$ , includes the substation  $s = s2 \dots S$ , where the harmonic filter shall not increase the harmonic voltage magnitudes  $U_{p,s,h}$ . For this substation group, the harmonic filter design shall not introduce the harmonic impedance shifts causing amplification above a threshold value.

For example, the task of the harmonic filter design can be formulated as that the harmonic voltage distortion is maintained below 70% of the IEC planning levels with the total component tolerances 10% in the substation group  $s1$ , i.e.  $U_{PL,k} = (1-0.1) \cdot 0.7 \cdot U_{IEC,k}$ , and not increased by more than 20% (and maintained below the IEC planning levels) in the substation group  $s2$ , for all operation conditions of the transmission grid included in the assessment.

#### 3.2 Harmonic tuning order

The harmonic voltage magnitudes  $U_{p,s,k}$  are normalized using the performance criteria,  $U_{PL,k}$ , as the base values:

$$u_{p,s,k} = \frac{U_{p,s,k}}{U_{PL,k}}, \quad k = 2 \dots K, \quad s = 1 \dots S, \quad p = 1 \dots P. \quad (2)$$

The harmonic tuning order  $n_{hp}$  is calculated by iterations using the normalized harmonic voltage magnitudes:

$$\begin{cases} n_{h,p,i+1} = \frac{\sum_{k=2}^K (k \cdot \sum_{s=s1}^{s2} (a_{p,s,k,i} \cdot u_{p,s,k,i}))}{\sum_{k=2}^K (\sum_{s=s1}^{s2} (a_{p,s,k,i} \cdot u_{p,s,k,i}))}, & \max(u_{p,s,k,i}) > 1 + \delta \\ n_{h,p,i+1} = n_{h,p,i}, & 1 < \max(u_{p,s,k,i}) \leq 1 + \delta \end{cases} \quad (3)$$

where  $k$  is the harmonic order ranging from 2 to  $K$ ,  $u_{p,s1,k}$  and  $u_{p,s2,k}$  are the maximum magnitudes of the normalized  $k^{\text{th}}$  harmonic voltage among the substation groups  $s1$  and  $s2$ , respectively,  $a_{p,s1,k}$  and  $a_{p,s2,k}$  are the participation factors of the substation groups  $s1$  and  $s2$ , respectively. The index  $i$  denotes the present iteration and  $i+1$  the next iteration.

The adjustment of the harmonic tuning order continues until the maximum magnitude of the normalized harmonic distortion is greater than  $1 + \delta_U$ . When the harmonic voltage distortion is reduced below this threshold, the harmonic tuning order gets locked on either the initial value calculated using the harmonic distortion before the harmonic filter or the value of the previous iteration  $i$ . Continuing adjustment does only inferior changes of the harmonic tuning order when the harmonic distortion is just above the performance criteria, which is why the adjustment discontinues and execution of the algorithm accelerates with locked harmonic tuning order. The threshold value is  $\delta_U \sim 1/3$  or smaller for the alignment.

The participation factors,  $a_{p,s1,k}$  and  $a_{p,s2,k}$ , include the following contributions:

- The harmonic voltage magnitudes in the substation group  $s1$  and group  $s2$  have the two different group weighting factors,  $\alpha_{s1}$  and  $\alpha_{s2}$ , with the largest weighting of the

substation group  $s1$ :  $\alpha_{s1} > \alpha_{s2}$ . Once assigned, these factors are kept unchanged for all operation scenarios  $p = 1 \dots P$ .

- The harmonic orders,  $k$ , to be dampened by the filter can have different design weighting factors,  $\beta_{p,k}$ , with the largest design weighting for the most predominant harmonic orders of the operation scenario  $p$ .
- The operational weighting factors  $\gamma_{p,s1,k}$  and  $\gamma_{p,s2,k}$  account for the violation occurrences of the  $k^{\text{th}}$  harmonic order planning level. These weighting factors depend on the harmonic voltage magnitudes and so on the operation conditions included in the harmonic filter design.

Thus, the participation factors are rewritten with the presented weighting factors:

$$a_{p,s1,k} = \alpha_{s1} \cdot \beta_{p,k} \cdot \gamma_{p,s1,k}, \quad a_{p,s2,k} = \alpha_{s2} \cdot \beta_{p,k} \cdot \gamma_{p,s2,k}. \quad (4)$$

The design weighting factors,  $\beta_{p,k}$ , can be either chosen at the start of the design process and kept unchanged for all operation scenarios or assigned individually for the different operation scenarios,  $p$ , included in the harmonic filter design. The assignment of  $\beta_{p,k}$  will be explained due the following sections.

In practical applications, the harmonic filter types, such as damped harmonic filters or double-tuned harmonic filters, and characteristic harmonic orders of the transmission grid shall be considered when applying Eq. (3). Further, the design weighting factors,  $\beta_{p,k}$ , can be assigned for groups of harmonic orders instead of for each harmonic order individually, such as the two design weighting factors  $\beta_{p,\{3,5,7\}}$  and  $\beta_{p,\{11,13\}}$  are applied for the grid with the 3<sup>rd</sup>, 5<sup>th</sup>, 7<sup>th</sup>, 11<sup>th</sup> and 13<sup>th</sup> characteristic harmonic orders to be addressed by the filter design algorithm.

Thus, the adjustable part of Eq. (3) is rewritten as:

$$\begin{aligned} n_{p,h1,i+1} &= \frac{\sum_{s=s1}^{s2} N_s}{\sum_{s=s1}^{s2} T_s}, \\ N_s &= \alpha_s \cdot \left( \beta_{p,\{3,5,7\}} \cdot \sum_{k=3,5,7} (k \cdot \gamma_{p,s,k,i} \cdot u_{p,s,k,i}) \right. \\ &\quad \left. + \beta_{p,\{11,13\}} \cdot \sum_{k=11,13} (k \cdot \gamma_{p,s,k,i} \cdot u_{p,s,k,i}) \right), \\ T_s &= \alpha_s \cdot \left( \beta_{p,\{3,5,7\}} \cdot \sum_{k=3,5,7} (\gamma_{p,s,k,i} \cdot u_{p,s,k,i}) \right. \\ &\quad \left. + \beta_{p,\{11,13\}} \cdot \sum_{k=11,13} (\gamma_{p,s,k,i} \cdot u_{p,s,k,i}) \right). \end{aligned} \quad (5)$$

for the design algorithm of a damped harmonic filter with the tuning order  $n_{p,h1}$  and:

$$\begin{aligned} n_{p,h1,i+1} &= \frac{\sum_{s=s1}^{s2} N_{s,3,5,7}}{\sum_{s=s1}^{s2} T_{s,3,5,7}}, \\ N_{s,3,5,7} &= \alpha_s \cdot \left( \beta_{p,\{3,5,7\}} \cdot \sum_{k=3,5,7} (k \cdot \gamma_{p,s,k,i} \cdot u_{p,s,k,i}) \right), \end{aligned} \quad (6)$$

$$T_{s,3,5,7} = \alpha_s \cdot \left( \beta_{p,\{3,5,7\}} \cdot \sum_{k=3,5,7} (\gamma_{p,s,k,i} \cdot u_{p,s,k,i}) \right).$$

$$n_{p,h2,i+1} = \frac{\sum_{s=s1}^{s2} N_{s,11,13}}{\sum_{s=s1}^{s2} T_{s,11,13}},$$

$$N_{s,11,13} = \alpha_s \cdot \left( \beta_{p,\{11,13\}} \cdot \sum_{k=11,13} (k \cdot \gamma_{p,s,k,i} \cdot u_{p,s,k,i}) \right),$$

$$T_{s,11,13} = \alpha_s \cdot \left( \beta_{p,\{11,13\}} \cdot \sum_{k=11,13} (\gamma_{p,s,k,i} \cdot u_{p,s,k,i}) \right).$$

for the design algorithm of a double-tuned filter with the tuning orders  $n_{p,h1}$  and  $n_{p,h2}$ .

### 3.3 Group weighting factor

The group weighting factors  $\alpha_{s1}$  and  $\alpha_{s2}$  are assigned at the start of the harmonic filter design algorithm. On the one hand, the assigned value  $\alpha_{s1}$  shall reflect that dampening of the harmonic voltage distortion in the substation group  $s1$  has the main priority of the design. On the other hand, the assigned value  $\alpha_{s2}$  shall account for how much the harmonic filter design may affect the harmonic voltage distortion in the substation group  $s2$ . For example,  $\alpha_{s1} = 1.0$  and  $\alpha_{s2} = 0.2$ , which will be kept constant during the entire design process.

### 3.4 Design weighting factor

The design weighting factors,  $\beta_{p,k}$ , account for which harmonic orders are predominant before establishment of the harmonic filter and need to be addressed by the designed harmonic filter, so that having the largest magnitudes of the normalized harmonic voltage distortion by Eq. (2). The design weighting factors are normalized to unity implying:

$$\sum_{k=2}^K \beta_{p,k} = 1. \quad (7)$$

The two options of how to assign the design weighting factors  $\beta_{p,k}$  are:

- “Manually” by inspection of the (measured or simulated) harmonic voltage distortion in the substations of the groups  $s1$  and  $s2$  and knowing harmonic characteristics of the transmission grid.
- By calculation using the (measured or simulated) harmonic voltage distortion before establishment of the harmonic filter.

For the option by calculation, the design weighting factor of the  $n^{\text{th}}$  harmonic order is:

$$\beta_{p,n} = \frac{\sum_{s=s1}^{s2} (\alpha_s \cdot \gamma_{p,s,n} \cdot u_{p,s,n})}{\sum_{k=2}^K (\sum_{s=s1}^{s2} (\alpha_s \cdot \gamma_{p,s,k} \cdot u_{p,s,k}))}, \quad (8)$$

with the index  $n = 2 \dots K$  representing the harmonic orders addressed by the harmonic filter design.

When the design weighting factors are assigned for groups of harmonic orders  $\beta_{p,\{3,5,7\}}$  and  $\beta_{p,\{11,13\}}$ , as in the above example, Eq. (8) is rewritten as:

$$\beta_{p,\{3,5,7\}} = \frac{\sum_{n=3,5,7} (\sum_{s=s1}^{s2} (\alpha_s \cdot \gamma_{p,s,n} \cdot u_{p,s,n}))}{\sum_{k=3,5,7,11,13} (\sum_{s=s1}^{s2} (\alpha_s \cdot \gamma_{p,s,k} \cdot u_{p,s,k}))}, \quad (9)$$

$$\beta_{p,\{11,13\}} = \frac{\sum_{n=11,13} (\sum_{s=s1}^{s2} (\alpha_s \cdot \gamma_{p,s,n} \cdot u_{p,s,n}))}{\sum_{k=3,5,7,11,13} (\sum_{s=s1}^{s2} (\alpha_s \cdot \gamma_{p,s,k} \cdot u_{p,s,k}))}.$$

The option by calculation allows assigning different design weighting factors for the different operation scenarios,  $p$ , included in the harmonic filter design. However, assigning of different factors is not strictly necessary, because the algorithm execution shall, at the end, result in a filter design being efficient for all included operation scenarios of the transmission grid.

### 3.5 Operational weighting factor

The operational weighting factors are:

$$\gamma_{p,s1,k} = \max(1, m_{p,s1,k}), \quad \gamma_{p,s2,k} = \max(1, m_{p,s2,k}), \quad (10)$$

with  $m_{p,s1,k}$  and  $m_{p,s2,k}$  being the numbers of violations of the  $k^{\text{th}}$  harmonic performance criteria in substations in the groups  $s1$  and  $s2$ . The operational weighting factors  $\gamma_{p,s1,k}$  and  $\gamma_{p,s2,k}$  are dependent from the harmonic voltages and, therefore, vary through the operation scenarios included in the harmonic filter design.

The smallest values of the weighting factors  $\gamma_{p,s1,k}$  and  $\gamma_{p,s2,k}$  are unity for not cancelling the  $k^{\text{th}}$  harmonic order contributions in Eq. (3) when the filter design eventually brings the  $k^{\text{th}}$  harmonic voltage distortion,  $U_{p,s,k}$ , below the performance criteria,  $U_{PL,k}$ , so that  $m_{p,s1,k} = m_{p,s2,k} = 0$  at no violation of the performance criteria.

### 3.6 Quality factor

The algorithm calculates the quality factor by iterations:

$$q_{F,p,i+1} = q_{F,p,i} \cdot \left( 1 + \min \left( c_{qF} \cdot \sum_{k=2}^K \left( \beta_{p,k} \cdot \sum_{s=s1}^{s2} \alpha_s \cdot u_{p,s,k,i} \right), \Delta q_F \right) \right), \quad (11)$$

$$q_{F\_MIN} \leq q_{F,p,i+1} \leq q_{F\_MAX},$$

where the quality factor of the next iteration,  $i+1$ , is calculated using the quality factor and the normalized harmonic voltage magnitudes of the present iteration,  $i$ .

The factor  $c_{qF}$  shall be less than unity and together with the factor  $\Delta q_F$  reflect how much the quality factor may step pr. iteration. For the harmonic filter design in the Danish 400 kV transmission grid, the values  $c_{qF} = 0.25$  and  $\Delta q_F = 1.15$  have been applied. However, the value  $c_{qF}$  is corrected by the rated reactive power step,  $\Delta Q_{HF}$ , avoiding dependency of the quality factor adjustment from the size of  $\Delta Q_{HF}$ .

When the harmonic voltage distortion is well dampened, such as  $1 < \max(u_{p,s,k,i}) < 1 + \delta_U$ , the change of the quality factor by Eq. (11) may become insignificant and replaced by a fixed step:

$$q_{F,p,i+1} = q_{F,p,i} + \Delta q_F, \quad |q_{F,p,i+1} - q_{F,p,i}| < \delta_{qF} \quad (11.a)$$

Usually, the values of the step and threshold are  $\delta_{qF} \ll \Delta q_F$ , with  $\Delta q_F$  being in a range of 0.25 and corrected by the rated reactive power step.

The quality factor,  $q_{F,p}$ , is calculated in the range from  $q_{F\_MIN}$  (assigned at the start of the algorithm) to  $q_{F\_MAX}$ , which shall prevent the algorithm from finding unproper numerical solutions. For the harmonic filter design in the Danish 400 kV transmission grid, the typical values have been:  $q_{F\_MIN} = 2$  and  $q_{F\_MAX} = 5$ .

For the Danish 400 kV transmission grid with the 3<sup>rd</sup>, 5<sup>th</sup>, 7<sup>th</sup>, 11<sup>th</sup> and 13<sup>th</sup> characteristic harmonic orders, the quality factor adjustment expression can be rewritten as:

$$q_{F,i+1} = q_{F,i} \cdot \left( 1 + \min c_{qF} \cdot \left( \beta_{3,5,7} \cdot \sum_{k=3,5,7} \left( \sum_{s=s1}^{s2} \alpha_s \cdot u_{s,k,i} \right) + \beta_{11,13} \cdot \sum_{k=11,13} \left( \sum_{s=s1}^{s2} \alpha_s \cdot u_{s,k,i} \right) \right) \right) \quad (12)$$

### 3.7 Rated reactive power

The algorithm adjusts the rated reactive power by iterations:

$$Q_{HF,p,i+1} = Q_{HF,p,i} + \Delta Q_{HF}, \quad (13)$$

$$Q_{HF\_MIN} \leq Q_{HF,p,i+1} \leq Q_{HF\_MAX},$$

where the rated reactive power of the next iteration,  $i+1$ , is calculated using the rated reactive power of the present iteration,  $i$ , and a fixed step  $\Delta Q_{HF}$ .

The rated reactive power,  $Q_{HF,p}$ , is in the range from  $Q_{HF\_MIN}$  (assigned at the start of the algorithm) to  $Q_{HF\_MAX}$ , which prevents finding excessive solutions.

### 3.8 Iteration discontinuing rules

As long as the harmonic voltage distortion reduces as the result of adjusted harmonic tuning orders or quality factor, the iteration process continues with adjustment of either the harmonic tuning orders or the quality factor.

When unacceptable increase of the harmonic voltage distortion is detected in the substation groups  $s1$  and  $s2$ :

- The harmonic tuning order iteration discontinues and reassigns the value of the previous iteration if caused by the harmonic tuning order adjustment of the iteration  $i+1$ :

$$n_{h,p,i+1} = n_{h,p,i} \quad (14)$$

- The quality factor iteration discontinues and reassigns the value of the previous iteration if caused by the quality factor adjustment of the iteration  $i+1$ :

$$q_{F,p,i+1} = q_{F,p,i} \quad (15)$$

Furthermore, the algorithm applies the adjustment efficiency margins  $\varepsilon_{nh}$  for the harmonic tuning order and  $\varepsilon_{qF}$  for the quality factor. Since the iterations of both harmonic tuning

order by Eq. (3) and quality factor by Eq. (11) apply the harmonic voltage magnitudes as the input signals, insignificant changes of the harmonic tuning order:

$$|n_{h,p,i+1} - n_{h,p,i}| < \varepsilon_{nh} \quad (16)$$

and quality factor:

$$|q_{F,p,i+1} - q_{F,p,i}| < \varepsilon_{qF} \quad (17)$$

imply that the  $i+1$  iteration of either harmonic tuning order or quality factor does not efficiently reduce the harmonic voltage distortion. In such cases, the iteration loop is discontinued and the adjusted design parameter keeps the  $(i+1)^{\text{th}}$  value. Typical values of the adjustment efficiency margins,  $\varepsilon_{nh}$  and  $\varepsilon_{qF}$ , are in a range of 0.001...0.01. The control condition Eq. (17) applies before conducting stepping by Eq. (11.a).

### 3.9 Alignment of included operation scenarios

Different  $(n-M)$ ,  $M \geq 0$ , operation conditions of the grid combined with different power transports representing the different operation scenarios,  $p = 1 \dots P$ , may have different magnitudes of the harmonic voltage distortion in the same substations, which leads to differences of the rated reactive power,  $Q_{HF,p}$ , harmonic tuning orders,  $n_{h,p}$ , and quality factor,  $q_{F,p}$ , found by the design algorithm for these operation scenarios.

The different design parameters,  $Q_{HF,p}$ ,  $n_{h,p}$ , and  $q_{F,p}$ , with  $p = 1 \dots P$ , shall be adjusted to the common design parameters,  $Q_{HF}$ ,  $n_h$ , and  $q_F$ , which work efficiently for all the included operation scenarios. The alignment algorithm is by iterations, with the initial iteration:

$$\begin{aligned} Q_{HF,j} &= \max(Q_{HF\_MIN}, \max(Q_{HF,p}) - \Delta Q), \\ n_{h1,j} &= \text{average}(n_{h1,p} |_{\max(Q_{HF,p})}), \\ q_{F,j} &= \max(q_{F,p} |_{\max(Q_{HF,p})}), \end{aligned} \quad (18)$$

with  $j = 1$  and  $p = 1 \dots P$ . In the initial iteration by Eq. (18), the rated reactive power is the maximum value among the rated reactive powers of the operation scenarios corrected by  $\Delta Q$  being in a range of 0 to a couple of steps  $\Delta Q_{HF}$ . The tuning harmonic orders use the average among the harmonic tuning orders for the designs with the maximum rated reactive powers. The quality factor uses the maximum among the quality factors for the designs with the maximum rated reactive powers.

During the alignment algorithm, the rated reactive power and the tuning harmonic orders are adjusted as:

$$\begin{aligned} Q_{HF,j+1} &= Q_{HF,j} + \Delta Q_{HF} |_{Q_{HF\_STOP}} \\ n_{h1,j+1} &= \frac{\sum_{p=1}^P (n_{h1,p,j} \cdot Q_{HF,p,j})}{\sum_{p=1}^P (Q_{HF,p,j})}, \\ q_{F,j+1} &= q_{F,j} \end{aligned} \quad (19)$$

with  $j$  being the present iteration and  $j+1$  the next iteration, until the harmonic filter design shall bring the harmonic voltage distortion below the performance criteria for all operation scenarios  $p = 1 \dots P$ .

The scenario specific harmonic tuning orders,  $n_{h1,p,j}$  are updated using Eq. (3), Eq. (5) and Eq. (6). Thus, the harmonic tuning order of the iteration  $j+1$ ,  $n_{h1,j+1}$ , uses the harmonic voltage magnitudes of the iteration  $j$  for all operation scenarios,  $p = 1 \dots P$ . The quality factor is kept unchanged through the iterations.

The alignment iterations by Eq. (19) discontinue if the rated reactive power reaches the maximum acceptable rating  $Q_{HF\_STOP}$ . In such case, if the harmonic filter design is still insufficient for dampening the harmonic voltage distortion in the substations of the group  $s1$  without increasing the distortion in the substations of the group  $s2$ , the connection substation of the harmonic filter has been wrongly chosen.

In such case, another connection substation shall be chosen and assessed using the presented algorithm.

In practice, several connection substation candidates will be preselected and assessed one by one for finding the most suitable connection substation of the harmonic filter. The Danish experience in connection with 400 kV UGC projects shows that the most suitable connection substations are found among the substations:

- With excessive harmonic distortion which shall be mitigated by the filter,
- With harmonic sources which significantly contribute to excessive harmonic distortion, or
- In closest proximity of the established UGC.

### 3.10 Linear or nonlinear inputs

The mathematical expressions of the harmonic tuning order by Eq. (3) and the quality factor by Eq. (11), Eq. (18) and Eq. (19) are linear because of using linear input signals, such as the (measured or simulated) harmonic voltage magnitudes. However, the presented algorithm does not exclude inputting nonlinear expressions of the harmonic voltage magnitudes, such as  $(u_{p,s,k})^N$  where  $s = 1 \dots S$  denotes the substations,  $k = 2 \dots K$  is the harmonic order,  $p = 1 \dots P$  is operation scenarios, and  $N \neq 1$  is the exponential order. Combinations of linear and nonlinear input signals are not excluded either.

The Danish experience is that linear input signals,  $u_{p,s,k}$ , work well with the presented mathematical algorithm and will be applied for presentation of the case study of the Eastern Danish 400 kV transmission grid in the following sections.

### 3.11 Decision making and process flow diagrams

The decision making on a new harmonic filter begins with identification of the operation scenarios,  $p = 1 \dots P$ , and incidents of excessive harmonic voltage distortion in such scenarios  $\{U_{p,s,k}\}$ , in the grid yet without the harmonic filter. In the Danish transmission grid, the practice applies the 95<sup>th</sup> weekly percentiles of the IEC planning magnitudes [5] as the



performance criteria. Evaluation of whether the  $k^{\text{th}}$  harmonic distortion violates the 95<sup>th</sup> weekly percentiles of the IEC planning level shall include the total duration of the operation scenarios with violated  $k^{\text{th}}$  harmonic planning magnitudes. If the performance criteria are violated in terms of the 95<sup>th</sup> weekly percentiles, then a mitigation solution is needed. The mitigation solution can be a new harmonic filter in a right connection substation with proper design parameters,  $Q_{\text{HF}}$ ,  $n_{\text{h1}}$ , and  $q_{\text{F}}$ .

The substations with and harmonic orders of excessive harmonic distortion are notified and the substation candidates for possible connection of the harmonic filter to be designed are chosen. The term “excessive” implies the harmonic distortion magnitudes which are either high but not violating or violating the performance criteria.

The harmonic filter design includes the two main algorithms which in general terms are shown in Fig. 1:

- The filter design algorithm conducted specifically for each operation scenario,  $p = 1 \dots P$ . This algorithm is shown in Fig. 1(a) and may result in  $P$  variants of the harmonic filter designs  $\{Q_{\text{HF},p}, n_{\text{h1},p}, q_{\text{F},p}\}$  due to differences of the grid operation scenarios. In the following, this will be called the design algorithm.
- The algorithm aligning the different  $P$  filter design variants into a common filter design  $\{Q_{\text{HF}}, n_{\text{h1}}, q_{\text{F}}\}$  fitted for all included operation scenarios, which is shown in Fig. 1(b). This will be called the alignment algorithm.

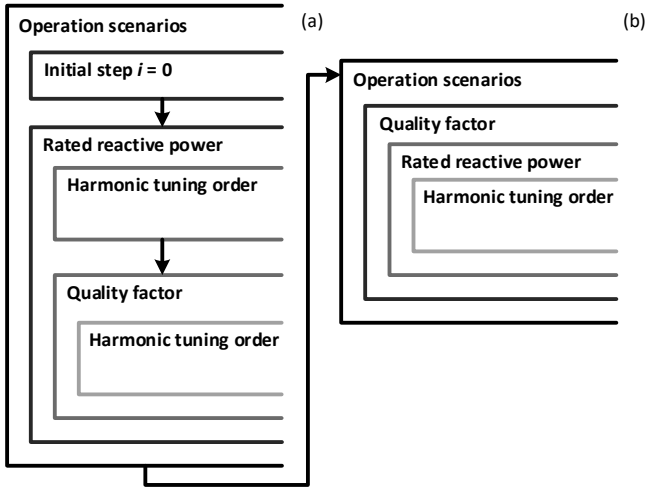


Fig. 1 Harmonic filter design algorithms: (a) – design algorithms for the different  $P$  operation scenarios, (b) – alignment algorithm leading to a common harmonic filter design. Each algorithm includes several iterations illustrated by  $\square$ .

### 3.12 Design algorithm and its process flow diagram

For the harmonic filter design, the performance criteria,  $U_{\text{PL},k}$ , are defined according to Eq. (1), now with inclusion of the design margins. The filter component tolerances [6],  $\delta_{\text{TOL}}$ , can be included in the design margins securing that detuning does not cause violation of the performance criteria during operation.

The substations  $s = 1 \dots S$  are divided into the two groups  $s1$  and  $s2$ . The group  $s1$  shall always include the connection substation of the new harmonic filter, the substations with violated performance criteria and, to some extent, the substations with high (but not violating the planning levels) harmonic distortion. The group  $s2$  shall include (but not restrict to) the remaining substations with high (but not violating the performance criteria) distortion, which are not in the group  $s1$ . The groups  $s1$  and  $s2$  shall not include the same substations. Here, the group weighting factors  $\alpha_{s1}$  and  $\alpha_{s2}$  are assigned and kept constant in both algorithms.

The process flow diagram of the design algorithm is shown in Fig. 2 (compare to the general-level diagram of Fig. 1(a) for identifying the iterations).

**3.12.1 Initial step:** Acquire and normalize using Eq. (2) the harmonic voltage magnitudes for the operation scenario  $p$ . If the harmonic voltage distortion for the operation scenario  $p$  does not violate the performance criteria, then a harmonic filter is not needed for this operation scenario. The acquired harmonic voltage magnitudes  $u_{p,s,k}$  are saved and reported to the alignment algorithm.

If violate, then the design weighting factors  $\beta_{p,k}$  are calculated using the harmonic voltage distortion and will be kept constant for this operation scenario. The initial values of the rated reactive power,  $Q_{\text{HF},p,i} = Q_{\text{HF\_MIN}}$ , harmonic tuning orders  $n_{\text{h1},p,i}$ , and quality factor,  $q_{\text{F},p,i} = q_{\text{F\_MIN}}$ , are assigned to the designed harmonic filter.

If the harmonic filter with the assigned parameters result in that the harmonic voltage distortion does not violate the performance criteria, then the filter design is completed. The harmonic voltage magnitudes and the filter design parameters  $\{u_{p,s,k}, Q_{\text{HF},p}, n_{\text{h1},p}, q_{\text{F},p}\}$  are saved and reported to the alignment algorithm. The design algorithm proceeds to the next operation scenario  $p + 1$ .

If still violates, the algorithm proceeds to the design iterations for the operation scenario  $p$ .

**3.12.2 Harmonic tuning order iteration:** The harmonic tuning order,  $n_{\text{h1},p,i+1}$ , is calculated using the acquired harmonic voltage magnitudes in the substation groups  $s1$  and  $s2$  from the previous iteration  $i$ . The rated reactive power,  $Q_{\text{HF},p,i+1}$ , and quality factor,  $q_{\text{F},p,i+1}$ , are locked. The iteration continues as long as the harmonic voltage magnitudes,  $u_{p,s,k,i+1}$ , get reduced but violate the performance criteria, and the change of the harmonic tuning order between iterations is greater than the threshold  $\epsilon_{n_{\text{h1}}}$ . The algorithm includes a measure breaking the iteration process if toggling is indicated.

If the harmonic voltage distortion stops violating the performance criteria, the filter design is completed. The harmonic voltage magnitudes and the filter design parameters  $\{u_{p,s,k}, Q_{\text{HF},p}, n_{\text{h1},p}, q_{\text{F},p}\}$  are saved and reported to the alignment algorithm. The design algorithm proceeds to the next operation scenario  $p + 1$ .



If the harmonic voltage distortion still violates the planning level, the algorithm proceeds to the quality factor iteration for the operation scenario  $p$ .

**3.12.3 Quality factor iteration:** The quality factor,  $q_{F,p,i+1}$ , is calculated using the acquired harmonic voltage magnitudes in the substation groups  $s1$  and  $s2$  and the quality factor from the previous iteration  $i$ . The rated reactive power,  $Q_{HF,p,i+1}$ , is locked but the harmonic tuning order,  $n_{h1,p,i+1}$ , is adjusted together with the quality factor. This simultaneous adjustment is made because the quality factor adjustment may shift the harmonic impedance characteristic of the grid and change the harmonic voltage distortion, which again may need an adjustment of the harmonic tuning order. The iteration continues as long as the harmonic voltage magnitudes,  $u_{p,s,k,i+1}$ , get reduced but violate the performance criteria, and the change of the quality factor between iterations is greater than the threshold  $\varepsilon_{qF}$ .

If the harmonic voltage distortion stops violating the performance criteria, the filter design is completed. The harmonic voltage magnitudes and the filter design parameters  $\{u_{p,s,k}, Q_{HF,p}, n_{h1,p}, q_{F,p}\}$  are saved and reported to the alignment algorithm. The design algorithm proceeds to the next operation scenario  $p + 1$ .

If the performance criteria are still violated and/or the quality factor reaches maximum  $q_{F\_MAX}$ , the algorithm proceeds to the rated reactive power step for the operation scenario  $p$ .

**3.12.4 Rated reactive power step:** When iterations of the harmonic tuning order,  $n_{h1,p,i}$ , and the quality factor,  $q_{F,p,i}$ , are forced into the above explained break criteria, the rated reactive power is stepped by  $Q_{HF\_STEP}$ .

If the harmonic voltage distortion stops violating the performance criteria, the filter design is completed. The harmonic voltage magnitudes and the filter design parameters  $\{u_{p,s,k}, Q_{HF,p}, n_{h1,p}, q_{F,p}\}$  are saved and reported to the alignment algorithm. The design algorithm proceeds to the next operation scenario  $p + 1$ .

If the rated reactive power reaches maximum  $Q_{HF\_MAX}$ , and the performance criteria are still violated, the algorithm proceeds to the next operation scenario  $p + 1$ , and reports the immediate results  $\{u_{p,s,k}, Q_{HF,p}, n_{h1,p}, q_{F,p}\}$  to the alignment algorithm. The filter design is marked as not completed.

**3.12.5 Operation scenarios:** The assessed operation scenarios are  $p = 1 \dots P$ . The design algorithm continues until all  $P$  operation scenarios are assessed.

### 3.13 Alignment algorithm and its process flow diagram

Once established, the harmonic filter will be in-service permanently because it is needed in the most operation conditions of the grid. The alignment algorithm shall result in the harmonic filter design fulfilling all foreseen operation conditions which are represented by the various operation scenarios,  $p = 1 \dots P$ . The process flow diagram of the

alignment algorithm is shown in Fig. 3 (compare to the general-level diagram of Fig. 1(b) for identifying iterations).

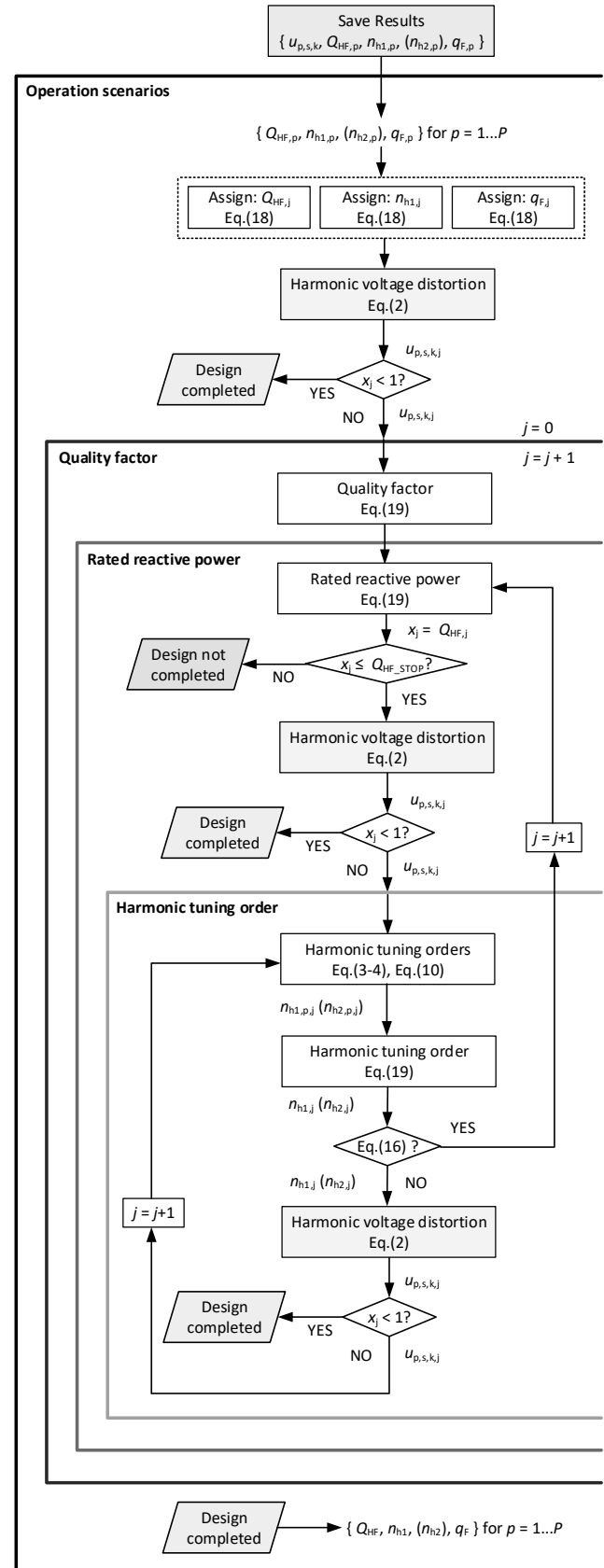


Fig. 3 Process flow diagram of the alignment algorithm with iterations.

In the start, the alignment algorithm receives the design parameters of the harmonic filter  $\{Q_{HF,p}, n_{h1,p}, q_{F,p}\}$  for the operation scenarios,  $p = 1 \dots P$ , from the design algorithm.

Among the operation scenarios, there can be scenarios with low harmonic voltage distortion which do not require harmonic filter. For such scenarios, the design parameters as zeros  $\{0, 0, 0\}$  are received from the design algorithm.

If the harmonic filter design starts from the alignment algorithm (and not from the design algorithm) such as fitting the predefined design parameters  $\{Q_{HF,p}, n_{h1,p}, q_{F,p}\}$  to comply with the operation scenarios,  $p$ , the input to the alignment algorithm is given as  $\{Q_{HF,p}, n_{h1,p}, q_{F,p}\}$  using the predefined parameters.

In the alignment algorithm, the harmonic filter will be enabled in all  $P$  operation scenarios, which also includes the scenarios with initial low harmonic voltage distortion not requiring harmonic filter.

**3.13.1 Operation scenarios (initial step):** Applying the inputs  $\{Q_{HF,p}, n_{h1,p}, q_{F,p}\}$  and Eq. (18), the algorithm calculates the initial rated reactive power, harmonic tuning orders, and quality factor  $\{Q_{HF,j}, n_{h1,j}, q_{F,j}\}$  of the common filter design. Applying the common filter design, the algorithm acquires and normalizes using Eq. (2) the harmonic voltage magnitudes in all  $S$  substations for all  $P$  operation scenarios. If the harmonic voltage distortion in all  $S$  substations for all  $P$  operation scenarios does not exceed the performance criteria, then the harmonic filter design is completed and the alignment algorithm is exited.

If exceeds, the algorithm proceeds to the design iterations adjusting the rated reactive power and harmonic tuning order.

**3.13.2 Quality factor:** The quality factor,  $q_{F,j}$ , will remain unchanged during the iterations.

**3.13.3 Harmonic tuning order iteration:** The harmonic tuning order,  $n_{h1,j+1}$  ( $n_{h2,j+1}$ ) is calculated using the harmonic voltage magnitudes in the substation groups  $s1$  and  $s2$  for all  $P$  operation scenarios of the previous iteration  $j$ . The iteration continues until the harmonic voltage magnitudes become smaller than the performance criteria for all  $P$  operation scenarios.

The iteration discontinues when the change of the harmonic tuning order between the iterations becomes smaller than a chosen threshold,  $\epsilon_{nh}$ . The algorithm includes also a measure breaking the iteration process if toggling is indicated.

**3.13.4 Rated reactive power:** When iterations of the harmonic tuning order,  $n_{h1,j}$ , discontinues, the rated reactive power is stepped by  $Q_{HF\_STEP}$ .

When the harmonic voltage distortion does violate the performance criteria, the filter design is completed with the

filter design parameters  $\{Q_{HF}, n_{h1}, q_F\}$  for all  $P$  operation scenarios.

If the rated reactive power reaches maximum  $Q_{HF\_STOP}$ , and the performance criteria are still violated, the alignment algorithm stops, and the filter design is marked as not completed. In such case, another connection substation should be investigated.

## 4 Transmission grid of Eastern Denmark

The DKE transmission grid includes the islands of Zealand, Lolland, Falster, and Moen. The grid is synchronous with the Nordic Countries and asynchronous with the Continental Europe, meaning asynchronous with the transmission grid of Western Denmark (DKW) which includes the peninsula of Jutland and the island of Funen. The DKE transmission grid includes the 400 kV, 220 kV (onshore and offshore) and 132 kV meshed grids.

The DKE 400 kV transmission grid is stylistically drawn in Fig. 4. DKE is HVAC connected to Sweden via the two 400 kV and the two 132 kV combined OHL and submarine cable connections. The two 400 kV connections to Sweden are between the substations Gørlose (GØR) and Hovegård (HVE) in DKE and Söderås (SÅNS) in Sweden.

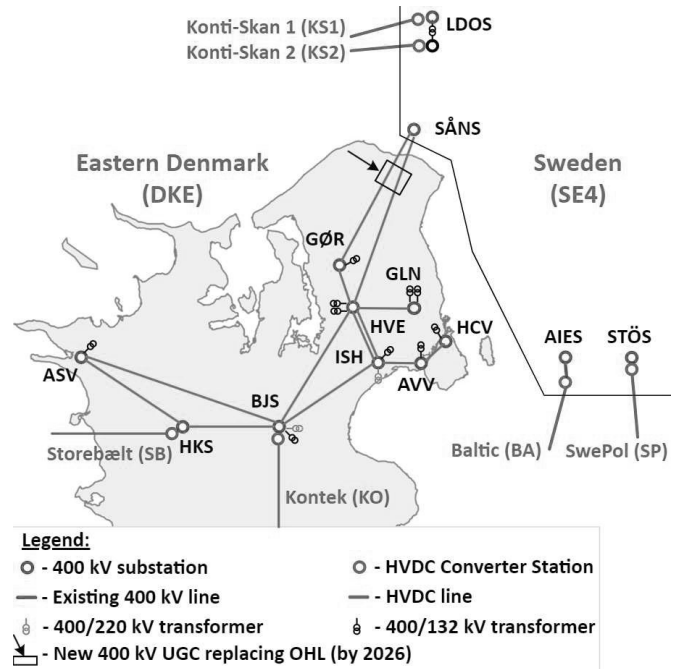


Fig. 4 400 kV transmission grid of Eastern Denmark (2021) with connection to and HVDC Converter Stations in Sweden (SE4) and marking a new 400 kV UGC replacing a section of an existing OHL (by 2026).

DKE is HVDC connected to Germany via the Kontek (KO) HVDC LCC connection and to DKW via the Storebælt (SB) HVDC LCC connection. Each HVDC connection is with 600 MW rating Converter Stations. DKE is also connected to Germany via the 220 kV cables, 220/150 kV offshore

transformation, 150 kV cables and the Back-to-Back VSC Converter Station in Bentwisch (400 MW, Germany) of the Kriegers Flak Combined Grid Solution (omitted in Fig. 4).

The Swedish Market Zone SE4 is in proximity of the DKE transmission grid and includes the 400 kV and 132 kV meshed transmission grids and several HVDC connections to the foreign systems: Konti-Skan 1 and 2 to DKW (KS1 and KS2, 740 MW in total), Baltic Cable (BA, 600 MW) to Germany, and SwePol (SP, 600 MW) to Poland. At the internal border, SE4 is HVAC connected to the Swedish Market Zone 3.

The simulation model of the DKE 400 kV transmission grid [1] with a new 11 km (double system, trace length) 400 kV UGC replacing an OHL section between the substations GØR and SÅNS, see Fig. 4, will be used as a case study for demonstration of the harmonic filter design algorithm. The simulation model represents the 400 kV, 220 kV and 132 kV grids of DKE using electro-geometrical data of the transmission lines (and to some extent electrical data of the 132 kV lines), electrical data of the 400 kV and 132 kV grids of SE4, and electrical data of the transformers, shunts and harmonic filters.

For simulation of the harmonic voltage distortion in the DKE 400 kV transmission grid, the model includes the harmonic emission sources of the six above-presented HVDC Converter Stations both in DKE and SE4 [1]. On the 400 kV level, these sources contribute primarily to the 11<sup>th</sup>, 13<sup>th</sup>, 23<sup>rd</sup> and 25<sup>th</sup> harmonic distortion.

The HVDC Converter Stations include harmonic filters, such as four filters of the SB in HKS and three filters of the KO in BJS. Data and operation of the harmonic filters of the Danish HVDC Converter Stations, such as which filters are in-service at a given power transport, are known from the vendor data, and operation for historical cases is available from SCADA. These harmonic filters are so far the only existing filters in the DK2 400 kV grid and purposed dampening of the 11<sup>th</sup>, 13<sup>th</sup>, 23<sup>rd</sup> and 25<sup>th</sup> harmonic distortion from the HVDC Converter Stations. Data and operation rules of the harmonic filters of the Swedish HVDC Converter Stations are provided by SvK for the purpose of the model development [1].

The model also includes the background harmonic distortion of the distributed sources present under the 132 kV transmission grid and propagating to the 400 kV substations through the 400/132 kV transformers. The distributed harmonic distortion exchanged with the Swedish grid is included as an aggregated source model behind the 400 kV substation SÅNS. In DKE, the distributed sources contribute mostly to the 3<sup>rd</sup>, 5<sup>th</sup>, and 7<sup>th</sup> harmonic distortion.

The simulation model of the DKE 400 kV transmission grid for harmonic assessment is successfully validated by the PQ measurements for various ( $n-M$ ),  $M \geq 0$ , operation conditions, power transports and number of the harmonic filters in-service of the HVDC Converter Stations [1]. The applied method makes the simulation model suitable for prediction of the

harmonic voltage distortion following establishment of a new connection in the 400 kV grid [1].

The harmonic assessment model and the harmonic filter design algorithm are implemented in the DIgSILENT PowerFactory simulation program which is the main software of Energinet for the transmission grid analysis.

#### 4.1 Impedance shift causing harmonic amplification

In July 2020, the operation conditions in the Eastern Danish transmission grid combining outage of a 400 kV line and a 400/132 kV transformer and operation of the harmonic filters of the KO HVDC Converter Station in the substation BJS have resulted in amplification of the 7<sup>th</sup> harmonic voltage distortion in the substation HKS.

The operation conditions before - case A, during - case B, and after the harmonic amplification - case C, are presented in Fig. 5. The measured harmonic voltage distortion (maximum of the three phase harmonic voltages with reference to the nominal-frequency three phase voltages) in the substation HKS with marking the three cases A, B, and C, is shown in Fig. 6.

Analysis of the operation conditions in Fig. 5 and the measured harmonic voltage distortion in Fig. 6 shows that the 7<sup>th</sup> harmonic voltage steps up when the 400 kV line between the substations BJS and HKS disconnects, and steps down to a low magnitude when an extra harmonic filter in HKS switches in-service and a harmonic filter in BJS switches out-of-service due to changed power transports of the SB and KO HVDC connections.

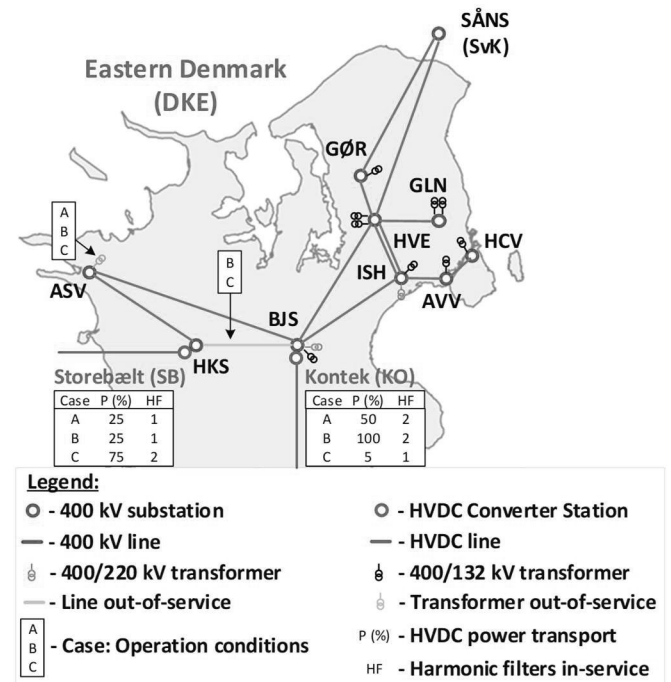


Fig. 5 400 kV transmission grid of Eastern Denmark with operation conditions: A - before, B - during, and C - after, amplification of the 7<sup>th</sup> harmonic voltage distortion in substation HKS.

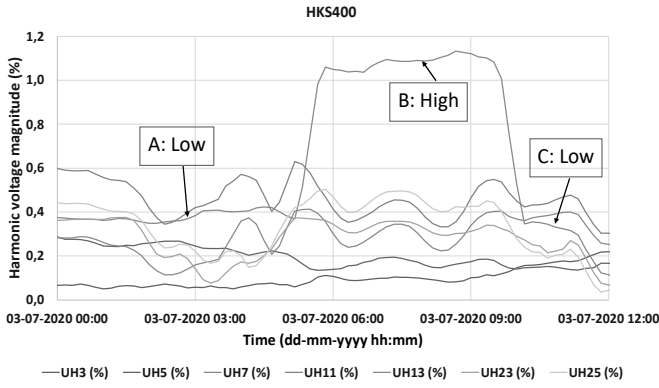


Fig. 6 Measured harmonic voltage distortion in the substation HKS at operation conditions: A - before, B - during, and C - after, causing amplification of the 7<sup>th</sup> harmonic voltage distortion. UH<sub>n</sub> means the  $n^{\text{th}}$  harmonic voltage in % of the nominal-frequency voltage.

Detailed analysis using the harmonic assessment model of the DKE 400 kV transmission grid reaches to the same conclusion, that the 7<sup>th</sup> harmonic voltage distortion in HKS increases in the operation conditions of case B and remains low in cases A and C. The magnitudes of other harmonic orders are not affected by the changed operation conditions through cases A, B and C. The simulated harmonic voltage magnitudes in the substation HKS are shown in Fig. 7.

The simulation model can overestimate the 5<sup>th</sup> harmonic voltage magnitudes in the summer periods such as in Fig. 7. This occurs because the 5<sup>th</sup> (and 7<sup>th</sup>) harmonic emission sources are tuned for the maximum 95<sup>th</sup> percentiles which for the 5<sup>th</sup> harmonic order are largest during the winter months (the 7<sup>th</sup> harmonic has no such seasonal dependency).

The simulated harmonic impedance characteristics in the substation HKS are plotted in Fig. 8. When the operation conditions change from case A to case B, the harmonic impedance characteristic increases around the 6.5<sup>th</sup> harmonic

order lifting the 7<sup>th</sup> harmonic impedance as well. This explains the increase of the 7<sup>th</sup> harmonic distortion in case B in comparison to case A.

When switching of the harmonic filters occurs such as in case C, the harmonic impedance characteristic shifts into lower harmonic orders reducing the 7<sup>th</sup> harmonic impedance magnitude. This result can explain the reduction of the 7<sup>th</sup> harmonic distortion in case C in comparison to case B.

The harmonic filters participated in switching are not tuned for the 7<sup>th</sup> harmonic order but may influence the 7<sup>th</sup> harmonic distortion due to the impedance shift in the meshed grid.

#### 4.2 New 400 kV UGC project and harmonic amplification

Replacement of an OHL section between the substations GØR, HVE and SÅNS with a new 400 kV UGC is scheduled by 2026, see Fig. 4. The new 400 kV UGC shall be a 11 km line length. A harmonic assessment has been part of the grid simulation studies conducted by Energinet for this UGC project and included around sixty operation scenarios combining different ( $n$ - $M$ ) operation conditions and power transports.

The harmonic assessment has found that establishment of the new UGC may significantly increase the 7<sup>th</sup> harmonic voltage distortion in DKE. In the substations HKS and ASV, which are located approx. 30...40 km from the new 400 kV UGC, the 7<sup>th</sup> harmonic voltage distortion may violate the IEC planning level, which for the 7<sup>th</sup> harmonic order is 2% of the nominal frequency voltage magnitude [5].

Influence of the new 400 kV UGC on the harmonic voltage distortion in the substation HKS is presented by the three cases from the harmonic assessment by Energinet. The three cases are depicted in Fig. 9. For distinguishing from the previous cases A, B, and C, the three cases of the new 400 kV UGC assessment are denoted D, E, and F.

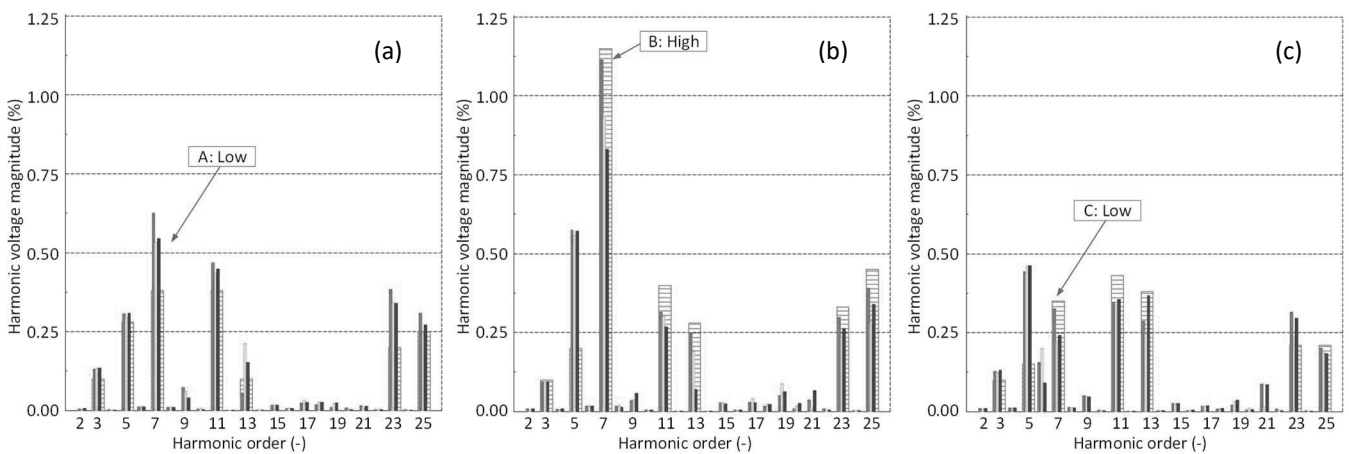


Fig. 7 Comparison of the simulated harmonic voltage magnitudes in the three phases A, B, and C marked by ■, ▨, and ■, to the measured harmonic voltage magnitudes marked by ▨, in the substation HKS for the operation conditions (a) - A, (b) - B, (c) - C with the 7<sup>th</sup> harmonic voltage distortion varying between low and high magnitudes.

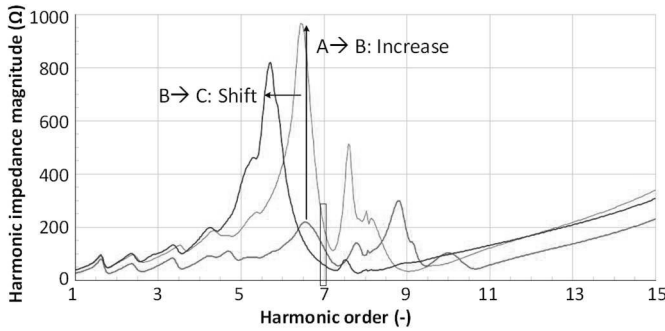


Fig. 8 Simulated harmonic impedance magnitudes in the substation HKS in cases: ■ - A, ■ - B, ■ - C, with notifications of increase and shift of the characteristics.

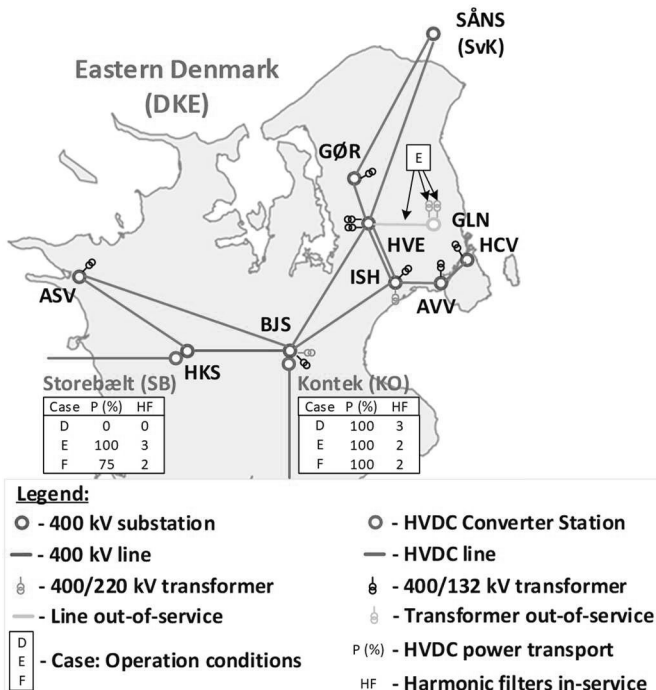


Fig. 9 400 kV transmission grid of Eastern Denmark with marking the three cases: D, E, and F.

Cases D and F are ( $n=0$ ) with different power transports and operation of the harmonic filters of the HVDC Converter Stations, while case E is with a 400 kV line and 400/132 kV transformers out-of-service disconnecting the 400 kV substation GLN. Before enabling the new 400 kV UGC, the three cases are with low magnitudes of the 7<sup>th</sup> harmonic voltage distortion.

The simulated harmonic voltage distortion and harmonic impedance magnitudes in the substation HKS before and after enabling the new 400 kV UGC are shown in Fig. 10 in % of the nominal frequency voltage magnitudes. The results before are compared to the measured harmonic voltage distortion for securing and demonstrating accurate initial magnitudes of the simulated harmonic distortion. The measured magnitudes are kept in the plots after enabling the 400 kV UGC for contrasting the magnitude changes.

The assessment shows that commissioning of the new 400 kV UGC will for the 7<sup>th</sup> harmonic voltage distortion result in:

- Almost unchanged magnitudes for case D,
- Significantly increased (reaching 70% of the IEC planning level) magnitude for case F, and
- Reaching 3.5% and violating the IEC planning level for case E.

Analysis of the harmonic impedance magnitudes supports the above presented results of direct simulations of the harmonic voltage distortion, such as the 7<sup>th</sup> harmonic voltage distortion increases when the harmonic impedance changes result in increased impedance magnitudes of the 7<sup>th</sup> harmonic order. However, the ratios of the 7<sup>th</sup> harmonic voltage magnitude increase are different from the ratios of the 7<sup>th</sup> harmonic impedance increase after enabling the 400 kV UGC. The ratio differences are because there is no (significant) 7<sup>th</sup> harmonic source in the substation HKS itself, while the 7<sup>th</sup> harmonic distortion propagating from other substations can be magnified through the adjacent connections and do not reach the substation HKS in-phase. This is the case of amplification of harmonic propagation.

The lessons learned from the above assessment are:

- Magnitudes of the harmonic voltage distortion in the present stage (meshed) grid are not always indicative for “guessing” on the harmonic voltage distortion in the next stage grid. Therefore, harmonic assessment must be conducted.
- Worst-case operation conditions are difficult to define using the harmonic distortion in the present stage grid as reference. Therefore, various operation conditions shall be included in harmonic assessment of the next stage grid.
- Both harmonic impedance characteristics by the passive grid data and harmonic emission sources are relevant for the harmonic assessment.
- The simulation results of harmonic voltage distortion and harmonic impedance (frequency scans) shall support each other.

## 5 Harmonic filter design and application

Using the present stage grid operation as reference, the total duration of the assessed operation scenarios with violated 7<sup>th</sup> harmonic distortion is within the 95<sup>th</sup> weekly percentiles. Thus, the 7<sup>th</sup> harmonic distortion will violate the IEC planning level, and a mitigation solution is required, such as establishment of a new harmonic filter.

In the following, the results of the harmonic filter design algorithm are presented for a high-pass 2<sup>nd</sup> order filter. A single line diagram of a high-pass 2<sup>nd</sup> order filter is shown in Fig. 11. The connection substation is GØR being in closest proximity of the new 400 kV UGC.

The substations GØR, HKS, ASV, HVE and BJS are assigned to the group s1, while the remaining substations AVV, HCV, GLN and ISH are in the group s2, see Fig. 12.

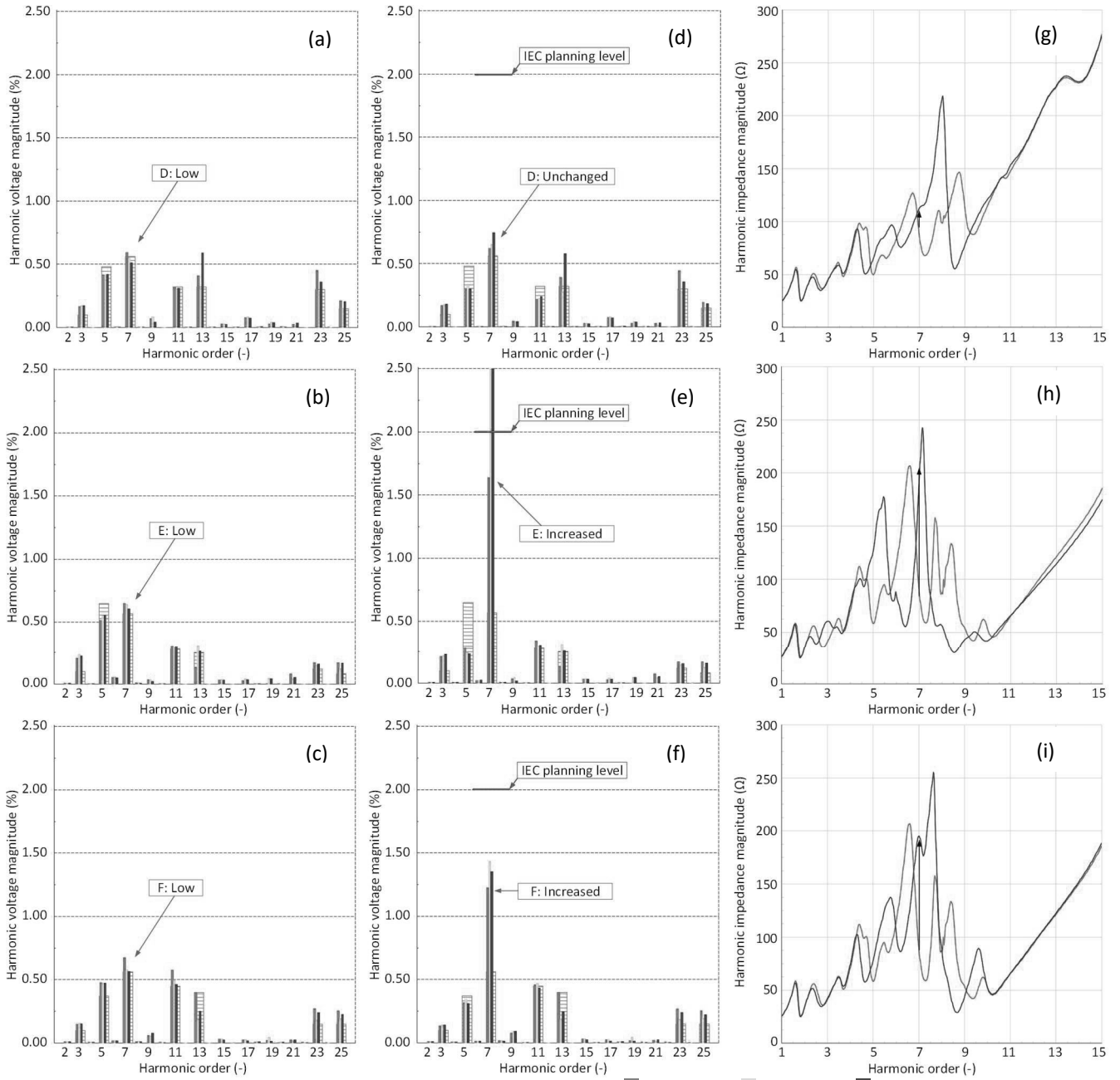


Fig. 10 Simulated harmonic voltage magnitudes the substation HKS: ■ - phase A, ■ - phase B, ■ - phase C, and the measured harmonic voltage magnitudes marked by ■. The operation conditions for before UGC: (a) – case D, (b) – case E, (c) – case F, and after UGC: (d) – case D, (e) – case E, breaking the shown scale and reaching 3.5% for the 7<sup>th</sup> harmonic order, (f) – case F. Simulated harmonic impedance magnitudes in the substation HKS in cases (g) – D, (h) – E, (i) – F: ■ - before, and ■ - after UGC. The arrows show impedance changes.

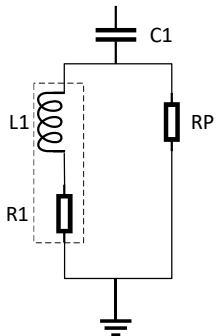


Fig. 11 Single line diagram of a high-pass 2<sup>nd</sup> order harmonic filter with the layout parameters  $C_1$  (capacitor),  $R_1$  and  $L_1$  (inductor), and  $R_p$  (parallel resistor).

The harmonic filter design algorithm is demonstrated using cases D, E and F of the previous presentation.

#### 5.1 Demonstration of design algorithm

The design algorithm begins with definition of the performance criteria. In this demonstration, the performance criteria are 70% of the IEC planning levels, meaning  $f_{PL,k} = 0.7$ , and use the total filter component tolerance of 10%, meaning  $\delta_{TOT} = 0.1$ , according to Eq. (1).



The algorithm proceeds with verification of the harmonic distortion before the harmonic filter is enabled and definition of the design weighting factors  $\beta_{p,\{3,5,7\}}$  and  $\beta_{p,\{11,13\}}$  for the operation scenarios  $p$ . The design weighting factors are assigned using Eq. (8-9) and shown in Table 1.

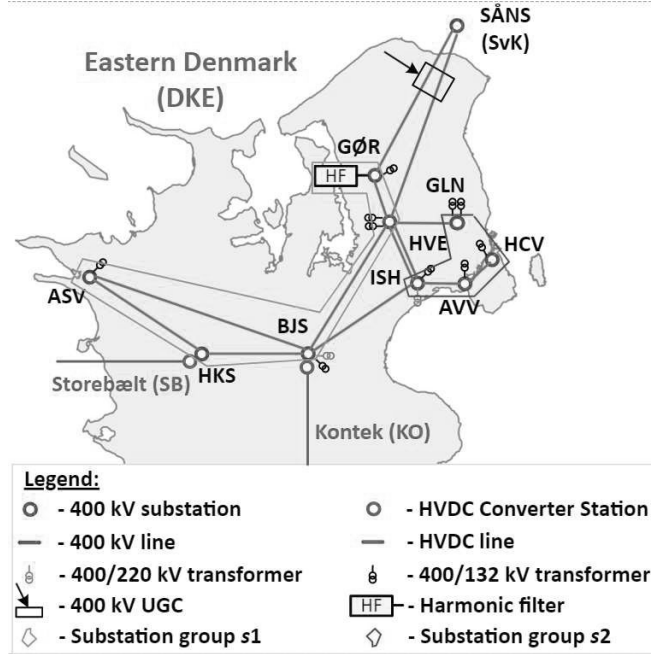


Fig. 12 Location of the assessed harmonic filter and the substation groups  $s1$  and  $s2$  in the map of the 400 kV transmission grid of Eastern Denmark.

Table 1 Design weighting factors

Scenario	$\beta_{p,\{3,5,7\}}$	$\beta_{p,\{11,13\}}$
D	0	0
E	0.92	0.08
F	0.69	0.31

For case D, the harmonic distortion is low and harmonic filter is not required, which is why the design weighting factors are zeros. For cases E and F, the largest design weighting factor is  $\beta_{p,\{3,5,7\}}$ , indicating high magnitudes of the 7<sup>th</sup> harmonic distortion. Thus, the primary target of the filter design shall be dampening of the 7<sup>th</sup> harmonic distortion. The harmonic filter shall also to most possible extent keep the 11<sup>th</sup> and 13<sup>th</sup> harmonic distortion below the performance criteria, which is indicated by the factor  $\beta_{p,\{11,13\}}$ . The design weighting factors remain unchanged through the whole filter design process.

For case E with the largest 7<sup>th</sup> harmonic distortion magnitudes among the three presented cases, the calculation progress of the filter design parameters  $\{Q_{HF,j}, n_{h1,j}, q_{F,j}\}$  is plotted in Fig. 13 and the harmonic voltage magnitudes in the  $s1$  group are plotted in Fig. 14.

Before iteration 1 the filter is not applied, which is why the filter design parameters in Fig. 13 are zeros and the 7<sup>th</sup>

harmonic distortion in Fig. 14 is excessive. The filter is enabled at iteration 1, with the initial parameters  $Q_{HF} = Q_{HF\_MIN} = 20$  MVar,  $q_F = q_{F\_MIN} = 2$ , and  $n_{h1} = 7.398$  calculated by Eq. (5).

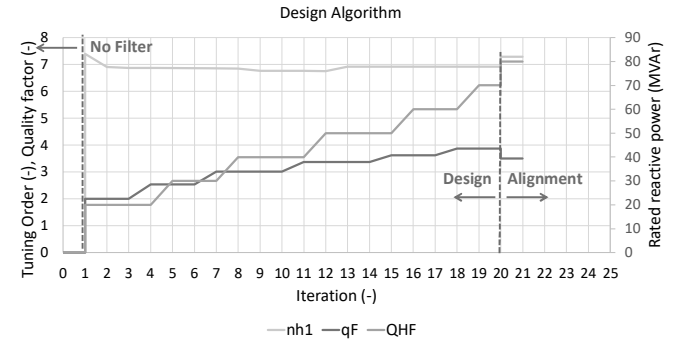


Fig. 13 Calculation progress of the filter design parameters  $Q_{HF}$ ,  $n_{h1}$ , and  $q_F$ , as functions of the design algorithm iteration,  $j$ .

During execution of the design algorithm, the harmonic tuning order is adjusted a couple times for each value of the rated reactive power and that of the quality factor.

The design algorithm stops when the harmonic voltage distortion is dampened to 100% of the performance criteria. In the presented case E, this is 100% for the 7<sup>th</sup> harmonic voltage in the substation HKS, see Fig. 14(a).

The results of the design algorithm for all three cases D, E, and F, are presented in Table 2.

Table 2 Design algorithm: Harmonic filter parameters

Scenario	$Q_{HF}$ (MVar)	$n_{h1}$ (-)	$q_F$ (-)
D	0	0	0
E	70	6.921	3.871
F	80	7.292	3.5

For case F, the design algorithm finds a harmonic filter with a larger than for case E rated reactive power, though the initial harmonic distortion is lower in case F than in case E. However, the quality factor is smaller for the filter design in case F than in case E. This result is because the numerical settings of the algorithm prioritize to get a smaller quality factor on a cost of a little larger reactive power since the harmonic filter is designed for the meshed grid. A larger quality factor is not wished because it will result in a steeper characteristic of the harmonic filter impedance magnitude. Hence there is a risk of increasing of other harmonic distortion for other orders (in other substations). The above statement is confirmed by a tendency of an increased 7<sup>th</sup> harmonic voltage magnitude in the harmonic filter connection substations GØR and reduced 7<sup>th</sup> harmonic voltage magnitudes in the other substations seen in Fig. 14 at the alignment step 21 when the quality factor is reduced from 3.871 to 3.5.

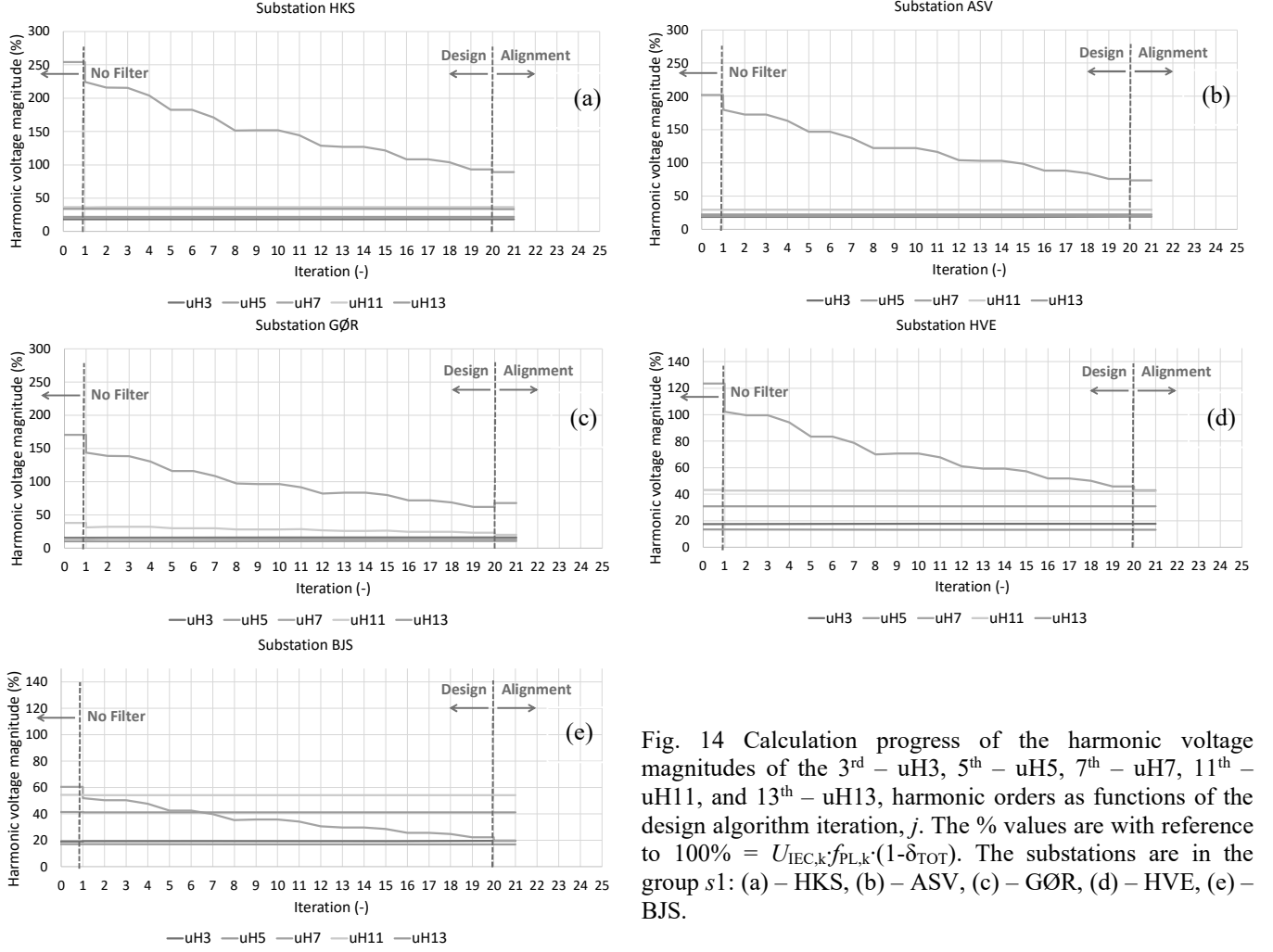


Fig. 14 Calculation progress of the harmonic voltage magnitudes of the 3<sup>rd</sup> – uH3, 5<sup>th</sup> – uH5, 7<sup>th</sup> – uH7, 11<sup>th</sup> – uH11, and 13<sup>th</sup> – uH13, harmonic orders as functions of the design algorithm iteration,  $j$ . The % values are with reference to  $100\% = U_{IEC,k} f_{PL,k} (1 - \delta_{TOT})$ . The substations are in the group  $s1$ : (a) – HKS, (b) – ASV, (c) – GØR, (d) – HVE, (e) – BJS.

### 5.2 Demonstration of alignment algorithm

A single iteration of the alignment algorithm is sufficient to dampen the 7<sup>th</sup> harmonic voltage distortion using the initial rated reactive power, harmonic tuning order and quality factor, in all substations, for the three operation scenarios D, E, and F. The initial (and final) parameters are calculated by Eq. (18). The results are shown in Table 3.

Table 3 Alignment algorithm: Harmonic filter parameters

Scenario	$Q_{HF}$ (MVar)	$n_{h1}$ (-)	$q_F$ (-)
Alignment	80	7.292	3.5

The plots for case E are found in Fig. 13 and Fig. 14. The alignment of the harmonic filter design results in further reduction of the 7<sup>th</sup> harmonic voltage distortion in all shown substations except of GØR. However, increase of the 7<sup>th</sup> harmonic distortion in GØR is not alerting.

## 6 Potential for active filtering/dampening

STATCOMs and HVDC VSC converters may deliver active filtering, when injecting a controlled harmonic current into the grid, or active dampening, when controlling the harmonic

impedance, with the goal of reducing the harmonic distortion in the grid [7]. Among requirements are that the power rating of the converter shall be sufficient for conducting active filtering or active dampening of harmonic distortion.

The presented algorithm of harmonic filter design can be utilized for control of the harmonic impedance,  $Z_k$ , of a power-electronic converter for reduction of the harmonic voltage distortion in the meshed transmission grid. This potential is evident from that the design algorithm finds different design parameters of the harmonic filter  $\{Q_{HF,p}, n_{h1,p} (n_{h2,p}), q_{F,p}\}$  for different operation conditions,  $p$ , before applying the alignment algorithm.

The measured harmonic voltage magnitudes in several substations of the meshed grid,  $u_{s,k}(t)$ , with  $t$  denoting time, are the inputs to the control. When the harmonic voltage magnitudes are acquired at the time  $t_i$ , the control shall:

- Calculate the design parameters  $Q_{HF}$ ,  $n_{h1}$  ( $n_{h2}$ ), and  $q_F$ , using the described algorithm. In fact, the rated reactive power,  $Q_{HF}$ , can be chosen knowing the converter rating available for the harmonic dampening and locked, while adjusting only the harmonic tuning order,  $n_{h1}$ , and quality factor,  $q_F$ . This would accelerate the calculation process.

- Convert the design parameters into the layout parameters using well known expressions. For the case of a high-pass 2<sup>nd</sup> order filter shown in Fig. 11, the layout parameters will be  $C_1$ ,  $L_1$ , and  $R_P$ :

$$C_1 = \frac{n_{h1}^2 - 1}{n_{h1}^2} \cdot \frac{Q_{HF}}{2 \cdot \pi \cdot f_{HF} \cdot U_{HF}^2},$$

$$L_1 = \frac{U_{HF}^2}{2 \cdot \pi \cdot f_{HF} \cdot (n_{h1}^2 - 1) \cdot Q_{HF}}, R_P = \frac{q_F \cdot n_{h1} \cdot U_{HF}^2}{(n_{h1}^2 - 1) \cdot Q_{HF}},$$

and  $U_{HF}$  is the nominal voltage.

- Calculate the impedance characteristic for the harmonic orders of interest,  $k$ , such as  $Z_k = Z_{C1} + (Z_{L1} || R_P)$  for the case of a high-pass 2<sup>nd</sup> order filter, with  $Z_{C1} = 1/(j \cdot \omega_k \cdot C_1)$  and  $Z_{L1} = j \cdot \omega_k \cdot L_1$ ,  $\omega_k = 2 \cdot \pi \cdot f_{HF} \cdot k$ , with  $f_{HF}$  being the nominal frequency.
- Elaborate the impedance characteristic  $Z_k$  in the converter control at time  $t_{i+1}$ .
- Acquire the harmonic voltage magnitudes at time  $t_{i+1}$  and repeat the above procedure.

The above-described method does not necessarily restrict to the high-pass 2<sup>nd</sup> order filter type and other filter types can be integrated in the active dampening control.

The strength of the proposed method is adjustment of the harmonic impedance characteristic of the converter using a fast algorithm and simultaneous accessing the measured harmonic distortion in several substations of the meshed grid.

## 7 Future trends of harmonic filtering

The presented algorithm is for design and operation of a harmonic filter connected to a given substation of the meshed transmission grid. The algorithm conducts and evaluates the filter design for the preselected substation candidates one at a time but does not predict in advance the most suitable connection substation among candidates. The procedure is an observational study which includes numerous harmonic distortion simulations using the presented algorithm, where the most suitable connection substation is decided from a subjective analysis of the design parameters of the harmonic filter and the harmonic voltage distortion.

Energinet and AAU Energy, Aalborg University, have started an Industrial PhD project [8] with the aim of developing analytical methods for determining harmonic propagation in meshed systems. As part of this study, it is expected that the methods can uncover whether it is possible to make an analytically harmonic assessment instead of or in parallel with observational studies for focused operating scenarios, and if so, under what conditions it is possible. The term 'focused' implies a reduced number of simulation cases selected according to the analytical approach. It is also expected that methods for determining the most suitable filter locations in the meshed transmission network can be developed.

Studies has shown that the propagation of harmonics can be interpreted as standing waves along transmission lines and that their terminal conditions determine the propagation [9].

When the propagation and the correlation between different stations is known, it is expected that it is possible to determine whether specific stations in a network are more susceptible to harmonics than others. This means that mitigating equipment could preferably be installed at these nodes or at nodes close to the most susceptible nodes. Based on this, there is an expectation that guidelines can be drawn up for choosing the most optimal mitigation strategy.

Another method that could be of general application is to determine the location of the mitigating equipment based on knowledge of the propagation of harmonics in the meshed network for several projects that entail changes in the structure of the network at once. One hypothesis is that if an optimal location in the network, which can advantageously absorb the change in harmonic emission caused by several projects, can be identified, the number of mitigating equipment can be minimized, and the overall cost can be reduced. An identification of optimal stations will be able to identify possible areas for the location of filters and hence, the selection of a set of stations  $S$  for the algorithm presented in this paper can be made on an informed basis.

## 8 Conclusion

The green transition of the electric energy generation and consumption as well as construction of the Energy Islands stipulates accelerated development of the transmission grid. In Denmark, the grid development shall for the most technically possible extent utilize the HVAC UGC instead of OHL. Increasing share of UGC has brought the resonances of the harmonic grid impedances down into the range of the harmonic distortion, which results in the harmonic distortion substantially increasing in some parts and reducing in other parts of the meshed transmission grid. Securing adequate levels of the power quality and harmonic mitigation are relevant for successful green transition.

This paper has presented an automated algorithm for design and operation of harmonic filters in the meshed transmission grid. The algorithm applies the harmonic voltage magnitudes in several substations as the inputs and returns the design parameters such as the rated reactive power, harmonic tuning order, and quality factor, for a given connection substation of the harmonic filter. Advantage of the algorithm is that it applies the magnitudes and do not need phase angles.

The algorithm works with several operation scenarios, which include combinations of different lines, transformers and shunt components out-of-service, and transports through the grid. Application of different operation scenarios result in that the algorithm returns some different design parameters, which in the alignment part of the algorithm are brought to common design parameters complying with all included operation scenarios.

Efficiency of the presented algorithm is demonstrated using the validated by PQ measurements simulation model of the Eastern Danish 400 kV transmission grid as a case study.

Replacement of a section of an existing 400 kV OHL with an UGC has resulted in significant systemwide increase of the 7<sup>th</sup> harmonic distortion in the 400 kV transmission grid. The harmonic assessment has shown violation of the IEC 7<sup>th</sup> harmonic planning level in the substations located approx. 30...40 km from the UGC location. Application of the harmonic filter designed by the algorithm has brought the harmonic voltage distortion under the performance criteria.

The presented algorithm has a potential for application in active filtering/dampening of the harmonic distortion as the algorithm proposes specific design parameters for different operation conditions of the grid. The design parameters can be converted to the harmonic impedance of the power electronic converter performing the active filtering/ dampening. Thus, the design parameters are calculated, and the harmonic impedance are controlled, using the measured harmonic voltage magnitudes in several substations as the inputs to the converter control system.

The development trend is evaluation of the most suitable connection substation of the harmonic filter using analytical methods instead of series of simulations assessing the connection substation candidates one at a time.

## 9 References

- [1] Akhmatov, V., Sørensen, M., Jakobsen, T., Hansen, C. S., Gellert, B. C., Bukh, B. S.: 'Harmonic distortion prediction method for a meshed transmission grid with distributed harmonic emission sources – Eastern Danish transmission grid case study', Paper WIW22-5, 21<sup>th</sup> Wind and Solar Integration Workshops, Oct. 12-14, 2022, Delft, The Netherlands.
- [2] Akhmatov, V., Hansen, C. S., Jakobsen, T.: 'Development of a harmonic analysis model for a meshed transmission grid with multiple harmonic emission sources', Paper WIW20-39, 19th Wind Integration Workshops, Nov. 11-12, 2020, Virtual Conference.
- [3] Kwon, J. B.: 'System-wide amplification of background harmonics due to the integration of high voltage power cables', Paper C4-305, CIGRÉ Session 2020.
- [4] Akhmatov, V., Hansen, C. S., Jakobsen, T.: 'Methods and results of harmonic simulation assessment of a reconstructed meshed transmission Grid with distributed harmonic emission sources', Paper WIW21-10, 20<sup>th</sup> Wind Integration Workshops, 29-30 Sept. 2021, Berlin, Germany.
- [5] IEC 61000-3-6: 'Electromagnetic Compatibility (EMC) – Part 3-6: Limits – Assessment of emission limits for the connection of distorting installations to MV, HV and EHV power systems'.
- [6] CIGRÉ, WG 14.30, 'Guide to The Specification and Design Evaluation of AC Filters for HVDC Systems', TB 139, April 1999.
- [7] Guest, E.: 'Active Filter Solutions for Reducing Harmonic Emissions by Wind Power Plants', PhD Thesis, Centre for Electric Power and Energy, Technical University of Denmark, July 2019.
- [8] Bukh, B. S.: 'Methods for harmonic analysis in meshed transmission systems.' [Online]. Available: <https://vbn.aau.dk/en/projects/methods-for-harmonic-analysis-in-meshed-transmission-systems>, accessed 24 May 2022.
- [9] Bukh, B. S., Bak, C. L., Faria da Silva, F.: 'Analysis of harmonic propagation in meshed power systems using standing waves', Paper C4-563, CIGRÉ Session 2022.